Reproducibility of the Realization of the Kilogram Based on the Planck Constant by the XRCD Method at NMIJ

Naoki Kuramoto, Shigeki Mizushima, Lulu Zhang, Kazuaki Fujita, Sho Okubo, Hajime Inaba, Yasushi Azuma, Akira Kurokawa, Yuichi Ota, and Kenichi Fujii

***Abstract*— The new definition of the kilogram based on the Planck constant was implemented in May 2019. The National Metrology Institute of Japan (NMIJ) will realize the new kilogram by the X-ray crystal density method using a ^{28}Si-enriched sphere. An international comparison of the realizations of the new kilogram by national metrology institutes was organized. As a participant in the comparison, the NMIJ realized the kilogram by the volume measurement and surface characterization of a ^{28}Si-enriched sphere. Details of the measurement results and the uncertainty evaluation of the realization are described. The comparison of the realization results with previous realization results in 2016 is also provided.**

***Index Terms*— Ellipsometry, kilogram, optical interferometry, Planck constant, silicon crystal, X-ray photoelectron spectroscopy (XPS).**

I. Introduction

IN MAY 2019, the International System of Units (SI) was essentially revised. Presently, all SI units are defined in terms of the seven defining constants [1]. In the new SI, the kilogram, the unit of mass, is defined by fixing the value of the Planck constant. Under the new definition, it is, in principle, possible for each national metrology institute to realize the kilogram independently. To ensure consistency among the realizations by national metrology institutes, an international comparison of the realizations based on the new definition, CCM.M-K8.2019, was organized by the Consultative Committee for Mass and Related Quantities. This comparison is an essential step toward the dissemination of the kilogram based on the individual realizations by each national metrology institute [2], [3].

The National Metrology Institute of Japan (NMIJ) will realize the new kilogram by using the X-ray crystal density (XRCD) method in the individual realization in the future. In this method, the kilogram at a nominal mass of 1 kg is realized using a ^{28}Si-enriched sphere [2], [4]. NMIJ has, therefore, participated in CCM.M-K8.2019 and has realized the kilogram by the XRCD method [5]. Details of the measurements for the realization at NMIJ are described in this article.

The evaluation of the reproducibility of the realization is also essential for the reliable individual dissemination of the kilogram [3]. The international equivalence of the realization by NMIJ was preliminarily confirmed in a pilot study in 2016 [6], in which the realizations based on a fixed value of the Planck constant by several national metrology institutes were compared. The reproducibility is, therefore, evaluated by comparing the results in this study with those in [4] and [6].

Manuscript received August 29, 2020; revised February 9, 2021; accepted February 16, 2021. Date of publication February 24, 2021; date of current version March 15, 2021. This work was supported in part by the Japan Society for the Promotion of Science through the Grant-in-Aid for Scientific Research (B) under Grant 20H02630. The Associate Editor coordinating the review process was Richard L. Steiner. *(Corresponding author: Naoki Kuramoto.)*

Naoki Kuramoto, Shigeki Mizushima, Lulu Zhang, Kazuaki Fujita, Sho Okubo, Hajime Inaba, Yasushi Azuma, Akira Kurokawa, Yuichi Ota, and Kenichi Fujii are with the National Metrology Institute of Japan/National Institute of Advanced Industrial Science and Technology, Tsukuba 305-8563, Japan (e-mail: n.kuramoto@aist.go.jp; s.mizushima@aist.go.jp; lulu.zhang@aist.go.jp; fujita.kazuaki@aist.go.jp; sho-ookubo@aist.go.jp; h.inaba@aist.go.jp; azuma-y@aist.go.jp; a-kurokawa@aist.go.jp; yuichi.ota@aist.go.jp; fujii.kenichi@aist.go.jp).

Digital Object Identifier 10.1109/TIM.2021.3061805

II. XRCD Method

In the XRCD method, the number N of Si atoms in an Si sphere is counted by measuring its volume V_S and lattice constant a. The number N is given by

$$N = 8V_S/a^3 \tag{1}$$

where 8 is the number of atoms per unit cell of crystalline silicon. The mass of the sphere m_S is therefore expressed by

$$m_s = Nm(\mathrm{Si}) \tag{2}$$

where $m(\mathrm{Si})$ is the mass of a single Si atom. The relationship between the Planck constant h and the mass of a single electron $m(\mathrm{e})$ is given by

$$R_\infty = \frac{m(\mathrm{e})c\alpha^2}{2h} \tag{3}$$

where c is the speed of light in the vacuum, α is the fine-structure constant, and R_∞ is the Rydberg constant. The mass of a single Si atom $m(\mathrm{Si})$ is related to $m(\mathrm{e})$ by

$$\frac{A_r(\mathrm{Si})}{A_r(\mathrm{e})} = \frac{m(\mathrm{Si})}{m(\mathrm{e})} \tag{4}$$

where $A_r(\mathrm{e})$ and $A_r(\mathrm{Si})$ are the relative atomic masses of electron and Si, respectively. Silicon consists of three stable isotopes, ^{28}Si, ^{29}Si, and ^{30}Si. The value of $A_r(\mathrm{Si})$ can, therefore, be determined by measuring the isotopic amount-of-substance fraction of each isotope. The relationship between $m(\mathrm{Si})$ and h is given by

$$\frac{h}{m(\mathrm{Si})} = \frac{1}{2}\frac{A_r(\mathrm{e})}{A_r(\mathrm{Si})}\frac{\alpha^2 c}{R_\infty}. \tag{5}$$

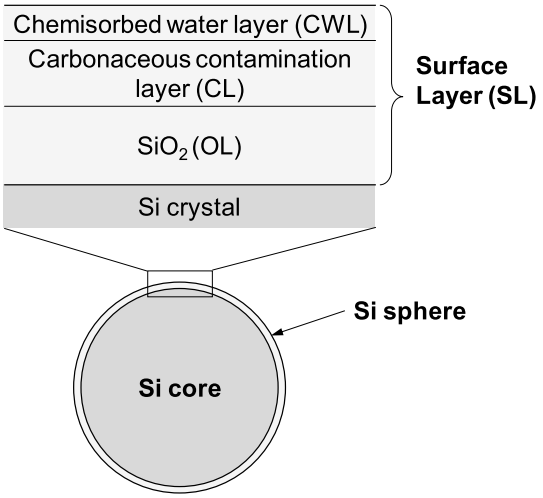

Fig. 1. Surface layer model for the characterization of the ^{28}Si-enriched sphere in vacuum.

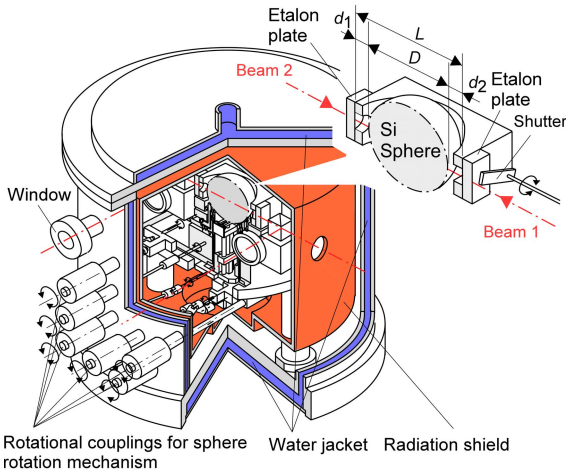

Fig. 2. Schematic of the optical interferometer used to measure the volume of the ^{28}Si sphere. The ^{28}Si-enriched sphere and the etalon are installed in a vacuum chamber equipped with an active radiation shield to control the sphere temperature [9].

By combining (1), (2), and (5), we can express the sphere mass m_s in terms of h as

$$m_s = \frac{2hR_\infty}{c\,\alpha^2}\frac{A_r(\mathrm{Si})}{A_r(\mathrm{e})}\frac{8V_s}{a^3}. \tag{6}$$

The sphere is covered by a surface layer with the main constituent of SiO_2 [4]. In addition, point defects are present inside the sphere [7]. Equation (6) should, therefore, be modified to

$$m_{\mathrm{core}} = \frac{2hR_\infty}{c\alpha^2}\frac{A_r(\mathrm{Si})}{A_r(\mathrm{e})}\frac{8V_{\mathrm{core}}}{a^3} - m_{\mathrm{deficit}} \tag{7}$$

where m_{core} and V_{core} are the mass and volume of the "Si core" part which excludes the surface layer, and m_{deficit} is the influence of point defects (i.e., impurities and self-point defects in the crystal) on the core mass [7]. The mass of the sphere m_{sphere} including the mass of the surface layer m_{SL} is given by

$$m_{\mathrm{sphere}} = m_{\mathrm{core}} + m_{\mathrm{SL}}. \tag{8}$$

The relative uncertainty of $R_\infty/(\alpha^2 A_r(\mathrm{e}))$ in (7) is estimated to be 4.0×10^{-10} [8] and the value of c is exactly defined in the SI [1]. In our previous studies, V_S, a, and $A_r(\mathrm{Si})$ of two 1 kg ^{28}Si-enriched spheres were measured with relative uncertainties of 2.0×10^{-8}, 5×10^{-9}, and 1.8×10^{-9}, respectively, [7], [9], [10]. The new kilogram definition based on h can, therefore, be realized with a relative uncertainty at a level of 10^{-8} using the ^{28}Si-enriched spheres at NMIJ.

III. Procedure of Realization of the New Kilogram

One of the two ^{28}Si-enriched spheres, AVO28-S5c, was used for the realization by NMIJ. Details of the sphere are described in [7], and the values of a, $A_r(\mathrm{Si})$, and m_{deficit} in (7) of the sphere were already measured [7]. The kilogram can, therefore, be realized by measuring V_s and m_{SL} of the sphere. Fig. 1 shows the surface model of the sphere under vacuum derived by the International Avogadro Coordination (IAC) project on the basis of the surface characterization using various analysis techniques [7]. In addition to the oxide layer (OL), a chemisorbed water layer (CWL) and a carbonaceous contamination layer (CL) exist. The CWL is a chemically absorbed water layer that is still present under ultrahigh-vacuum conditions. The CL is a carbonaceous layer formed by different adsorbed gases and contaminants originating from the environment during the measurement, handling, storage, and cleaning of the sphere. These layers are hereinafter collectively referred to as the surface layer (SL). For the surface characterization in this study, the thickness and mass of the SL were evaluated using an X-ray photoelectron spectroscopy (XPS) system and a spectroscopic ellipsometer. For the core characterization, an optical interferometer was used to measure the sphere volume. A phase shift is introduced to the reflection of the light beam on the sphere surface. The volume measured by the interferometer is, therefore, "apparent volume," which is slightly different from the core volume. The apparent volume should be corrected for the phase shift to obtain the core volume on the basis of the surface characterization.

A. Optical Interferometer

Fig. 2 shows a schematic drawing of the optical interferometer used to determine the volume of the ^{28}Si sphere by optical frequency tuning [9], [10]. A Si sphere is placed in a fused-quartz Fabry–Perot etalon. The sphere and etalon are installed in a vacuum chamber equipped with an active radiation shield to control the sphere temperature. The pressure in the chamber is reduced to 10^{-2} Pa. A laser beam from an external cavity diode laser is split into two beams (Beam 1 and Beam 2). They are reflected by mirrors toward opposite sides of the etalon. The light beams reflected from the inner surface of the etalon plate and the adjacent surface of the sphere interfere to produce concentric circular fringes. These are projected onto charge coupled device (CCD) cameras. The

fractional fringe order of interference for the gaps between the sphere and the etalon, d_1 and d_2, are measured by phase-shifting interferometry. The sphere diameter D is calculated as $D = L - (d_1 + d_2)$, where L is the etalon spacing. To determine L, the sphere is removed from the light path by a lifting device installed underneath the sphere, and Beam 1 is interrupted by a shutter. Beam 2 passes through a hole in the lifting device, and the beams reflected from the two etalon plates produce fringes on a CCD camera. The fringes are also analyzed by phase-shifting interferometry. The volume is determined from the diameter measured in many different directions. The required phase shifts in the phase-shifting interferometry are produced by changing the optical frequency of the diode laser. The optical frequency is controlled on the basis of the optical frequency comb, which is used as the national length standard of Japan [11], [12]. Details on the volume measurement are given in [9] and [10].

B. XPS System

The main component of the XPS system is ULVAC-Phi 1600C equipped with a monochromatic Al Kα X-ray source. The pressure in the measurement chamber is reduced to 5×10^{-7} Pa. A manipulator with five-axis freedom is installed in the chamber to realize the rotation of the sphere around the horizontal and vertical axes for the mapping of the entire surface. Details of the XPS system are given in [13].

C. Spectroscopic Ellipsometer

The main component of the spectroscopic ellipsometer is Semilab GES5E. Its spectral bandwidth ranges from 250 to 990 nm. The ellipsometer and an automatic sphere rotation system are integrated into a vacuum chamber to characterize the surface layer in the vacuum, where the pressure is reduced to 1×10^{-3} Pa. The ellipsometric measurement is carried out over the entire sphere surface using the automatic sphere rotation system. Details of the ellipsometer are provided in [14].

IV. Results of the Realization Experiment

A. Measurement Sequence

From September to October 2019, the volume was measured using the optical interferometer. The surface was characterized with the XPS system from November to December 2019 and the ellipsometer in January 2020.

B. Cleaning the Sphere

Before the volume measurement using the interferometer, the sphere was cleaned by the same procedure as that used by NMIJ in the international comparison of the diameter measurement of a 1 kg Si sphere in the IAC project [15] and for the pilot study of the realization of the kilogram [4]. In the first step of the procedure, the sphere was washed with a dilute aqueous solution of a detergent, during which the sphere was rotated between the hands wearing nitrile gloves. Next, the sphere was placed under a stream of water purified by the Milli-Q Integral system (Merck KGaA). Finally, ethanol was poured over the sphere. After cleaning, the sphere was stored in a clean booth overnight. The gloves were also dried in the booth and were used to install the sphere in each apparatus.

Mizushima *et al.* [16] reported that the mass of the sphere slightly decreased by the cleaning. To eliminate this effect of cleaning on the realization, the sphere was cleaned only before the volume measurement using the optical interferometer.

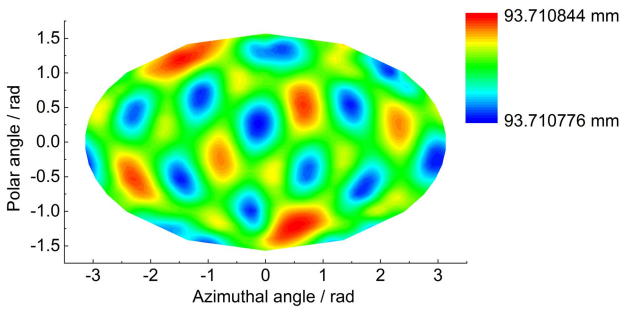

Fig. 3. Mollweide map projection of the distribution of the diameter measured from the 145 directions for AVO28-S5c.

C. Volume Measurement Using Optical Interferometer

A sphere rotation mechanism installed under the sphere was used to measure the diameter from many different directions. The measurement directions were based on 145 directions that are distributed nearly uniformly on the sphere surface [10]. The temperature of the sphere was measured using small platinum resistance thermometers (PRTs) that were calibrated using temperature fixed points in the International Temperature Scale of 1990 (ITS-90). The measured diameters were converted to those at 20.000 °C using the thermal expansion coefficient of the ^{28}Si-enriched crystal [17]. Fig. 3 shows the Mollweide map projection of the distribution of the diameter measured from the 145 directions, where the deviation from the mean diameter is enhanced. The peak-to-valley value of the diameter was 69 nm.

The measurement from the 145 directions was performed ten times. The total number of measurement directions was, therefore, 1450. Between each set of 145 directions, the sphere was rotated to distribute the starting point of each set of measurements to the vertices of a regular dodecahedron. Because the ten directions defined by the vertices of a regular dodecahedron are distributed equally, this procedure distributed all of the measurement points as uniformly as possible. The experimental standard deviation of the mean diameter was estimated to be 0.15 nm.

The measured diameter and volume are the apparent diameter and volume, respectively, which are not corrected for the phase shift due to the surface layer. Table I shows the uncertainty budget of the determination of the apparent volume V_{app}. The apparent volume was determined to be 430.891 2887(77) $\times 10^{-6}$ m^3 with a relative uncertainty of 1.8×10^{-8}. The largest uncertainty source is the phase correction due to the diffraction effect [18]. Another large uncertainty source is the interferogram analysis. The uncertainty contribution from this source to the apparent diameter measurement was estimated to be 0.1 nm. Details of this source are given in Section V-C of this article. Details of the results of the apparent volume measurement in this work are provided in [19].

TABLE I

UNCERTAINTY BUDGET IN THE DETERMINATION OF THE APPARENT VOLUME, V_{APP}, OF THE ^{28}Si SPHERE AT 20.000 °C AND 0 Pa

Uncertainty source	Standard uncertainty	Relative standard uncertainty in V_{app} / 10^{-9}
Sphere temperature	0.62 mK	4.8
Interferogram analysis	0.1 nm	3.4
Effect of Gouy phase shift	0.5 nm	16.0
Standard deviation of the mean diameter	0.15 nm	4.8
Relative combined standard uncertainty		17.8

D. Surface Characterization by XPS

The XPS spectra were measured at 52 points distributed nearly uniformly on the sphere surface. The 52 measurement points were defined by dividing the sphere surface into small cells of equal areas, and the measurement points were distributed individually in each cell [4].

1) Oxide Layer: The thickness of the OL was determined by analyzing the XPS Si 2p core-level spectra, in which peaks corresponding to the SiO_2 layer and the interfacial OL (Si_2O_3, SiO, and Si_2O) were observed. For rigorous evaluation of the OL thickness, accurate values of the attenuation lengths for the Si 2p electrons in SiO_2, Si_2O_3, SiO, and Si_2O were determined using SI-traceable X-ray reflectometry (XRR) system at NMIJ [20] using Si flat samples with different thicknesses of thermal SiO_2. Details of the determination of the attenuation lengths and the thickness of each layer are summarized in [13]. The OL thickness was determined as the sum of each OL. The average OL thickness at the 52 points was estimated to be 1.26 nm with a standard uncertainty of 0.067 nm.

2) Carbonaceous CL: In the XPS C 1s core-level spectra, peaks corresponding to the C–C/H and C–O bonds were observed. The peaks were estimated to be from ethanol and hydrocarbon. The thickness of the CL d_{CL} in Fig. 1 was, therefore, determined on the assumption that the CL was composed of an ethanol sublayer and a hydrocarbon sublayer. For the determination of the thickness of each sublayer, the densities of the ethanol and hydrocarbon sublayers were estimated to be 0.79(20) and 0.99(20) g/cm^3, respectively, where the large uncertainties were attributed because of the lack of sufficient information to clarify the chemical composition of the CL. The average thicknesses of the ethanol and hydrocarbon sublayers at the 52 points were estimated to be 0.46(7) and 0.35(5) nm, respectively. From these results, d_{CL} was estimated to be 0.81(9) nm. In addition, the density of the CL was estimated to be 0.88(14) g/cm^3 by considering the thickness and density of each sublayer. Details of the procedure to determine the CL thickness are given in [4].

E. Surface Characterization by Ellipsometry

First, the measurement was performed at the same 52 points used for the XPS measurement for the calibration of the ellipsometer using the results of XPS. For the calibration, the following equation was used:

$$d_{XPS} = d_{SE} + c \tag{9}$$

where d_{XPS} is the OL thickness measured by XPS, d_{SE} is the OL thickness measured by ellipsometry on the basis of the surface model of a SiO_2 layer on a Si substrate, and c is the calibration constant. c was determined from the average values of d_{XPS} and d_{SE} measured at the 52 points. After the calibration, the ellipsometric measurement was performed at 812 points distributed nearly uniformly on the sphere surface [4], and the measured d_{SE} was corrected by c. The measurement at the 812 points was repeated three times, and the total number of measurement points was 2436. Between sets of measurements at the 812 points, the sphere was oriented to distribute all the measurement directions as uniformly as possible. The average OL thickness on the 2436 points was estimated to be 1.26 nm. The standard deviation of the mean of d_{OL} for the three sets of measurements was 0.01 nm.

By combining the results of the surface characterization by ellipsometry and XPS, the OL thickness was estimated to be 1.26(68) nm. This result is summarized in Table II with those of the CL and CWL. The thickness of the CWL was estimated from the water adsorption coefficient on a silicon crystal surface reported by Mizushima [21].

TABLE II

MASS, THICKNESS, AND DENSITY OF SURFACE LAYERS IN VACUUM

Layer	Thickness / nm	Density / g cm^{-3}	Mass / μg
OL	1.26(7)	2.2(1)	76.5(5.4)
CL	0.81(9)	0.88(14)	19.6(3.8)
CWL	0.28(8) [a]	1.0(1) [a]	7.7(2.3)
SL			103.8(7.0)

[a] Values from [7].

V. SPHERE MASS

A. Mass of the Surface Layer

The mass of the surface layer m_{SL} is given by

$$m_{SL} = m_{OL} + m_{CL} + m_{CWL} \tag{10}$$

where m_{OL}, m_{CL}, and m_{CWL} are the masses of the OL, CL, and CWL, respectively. The masses were calculated from the thickness and density of each layer. The calculated masses are summarized in Table II. The total mass of the surface layer was estimated to be 103.8(7.0) μg.

B. Mass of the Sphere Core

The core mass m_{core} was derived from the core volume V_{core} using (7). To determine V_{core} from the apparent mean diameter measured using the optical interferometer, the total phase retardation on reflection at the sphere surface, δ, was calculated from the thickness and the optical constants of each layer [18]. Details of the optical constants of each layer are provided in [4]. The phase shift on reflection ($\delta - \pi$) was estimated to be −0.0459(26) rad. The effect of this phase

TABLE III
UNCERTAINTY BUDGET OF THE CORE MASS m_{core}

Uncertainty source	Value	Relative standard uncertainty in m_{core}	Source
Speed of light in vacuum, c	299 792 458 m s^{-1}	0	[22]
Planck constant, h	$6.626\,070\,15 \times 10^{-34}$ J s	0	[22]
Fine-structure constant, α	$7.297\,352\,5693(11) \times 10^{-3}$	3.0×10^{-10}	CODATA2018 [8]
Rydberg constant, R_∞	$1.097\,373\,156\,8160(21) \times 10^{7}$ m^{-1}	1.9×10^{-12}	CODATA2018 [8]
Relative atomic mass of silicon, A_{r}(Si)	27.976 970 09(15)	5.4×10^{-9}	[7]
Relative atomic mass of electron, A_{r}(e)	$5.485\,799\,090\,65(16) \times 10^{-4}$	2.9×10^{-11}	CODATA2018 [8]
Core volume, V_{core}	$430.\,891\,2877(77) \times 10^{-6}$ m^3	1.8×10^{-8}	This work
Lattice parameter, a	$543.099\,623\,80(97) \times 10^{-12}$ m	5.5×10^{-9}	[7], [23], this work
Mass deficit due to impurities and vacancies, m_{deficit}	3.8(3.8) µg	3.8×10^{-9}	[7]
Core mass, m_{core}	999.698 334(20) g	2.0×10^{-8}	

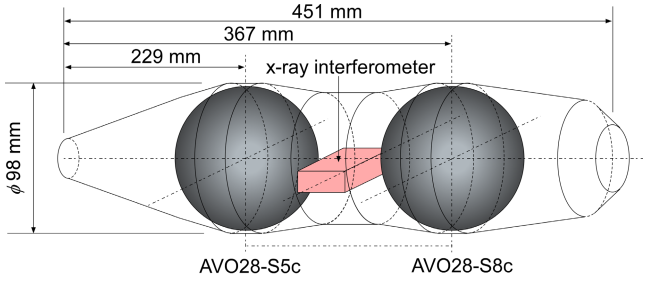

Fig. 4. Locations of the two ^{28}Si-enriched spheres, AVO28-S5c and AVO28-S8c, and the XINT in the AVO28 crystal.

shift on the gap measurement Δd was 2.31(13) nm. This means that the actual diameter including the surface layer is larger than the apparent diameter by 4.63(26) nm. The actual diameter D_{actual} is, therefore, obtained as $D_{\mathrm{actual}} = D_{\mathrm{app}} + 2\,\Delta d$. The phase shift correction to obtain the Si core diameter from the apparent diameter, Δd_0, was determined as $\Delta d_0 = 2\,(\Delta d - d_{\mathrm{total}})$, where d_{total} is the sum of the thicknesses of the layers. The value of Δd_0 was estimated to be $-0.072(53)$ nm. The Si core diameter D_{core} was determined to be 93.710 811 11(56) mm from $D_{\mathrm{core}} = D_{\mathrm{app}} + \Delta d_0$. The core volume of the sphere, V_{core}, was estimated as $V_{\mathrm{core}} = (\pi/6) D_{\mathrm{core}}^3$ to be $430.891\,2877(77) \times 10^{-6}$ m^3 with a relative uncertainty of 1.8×10^{-8}.

From V_{core}, the core mass m_{core} was derived to be 999.698 334(20) g with a relative uncertainty of 2.0×10^{-8} by using (7). Table III shows the uncertainty budget of the determination of m_{core}. The largest uncertainty source is the core volume determination using the optical interferometer.

The relative atomic mass of silicon A_{r}(Si) and the mass deficit due to impurities and vacancies of the sphere, m_{deficit}, were determined to be 27.976 970 09(15) and 3.8(3.8) µg, respectively, by the IAC in 2015 [7], and no new measurement of these two parameters of AVO28-S5c was performed. These values were, therefore, used to determine m_{core} in this study.

As to the lattice parameter a, the Istituto Nazionale di Ricerca Metrologica (INRiM, Italy) determined the lattice constant of the X-ray interferometer (XINT) sample of the AVO28 crystal to be 543.099 6197(96) pm [7]. Fig. 4 shows the locations of the XINT sample and the spheres in the AVO28 crystal. Because contaminants such as carbon and nitrogen strain the crystal lattice, a contamination gradient in the crystal makes the lattice parameter of the sphere different from that of the XINT. To measure the contamination gradient, samples were taken from the AVO28 crystal around the sphere. The impurity concentrations in the samples were measured by infrared spectroscopy. The lattice constant of AVO28-S5c was then estimated to be 543.099 6219(10) pm taking into account the difference in contamination concentration between the sphere and the XINT [7]. In 2017, the lattice parameter of the XINT sample was corrected to 543.099 621 61(93) pm taking into account the rigorous evaluation of the diffraction of the laser beam and the surface stress [23]. On the basis of this correction, the lattice parameter of AVO28-S5c was also corrected to 543.099 623 80(97) pm, which was the value used to determine m_{core} in this study.

C. Mass of the Sphere

From the core mass m_{core} and the mass of the surface layer m_{SL}, the mass of the sphere including the surface layer in the vacuum, m_{sphere}, was determined to be 999.698 438(21) g with a relative uncertainty of 2.1×10^{-8} using (7) and (8). Table IV shows the uncertainty budget of m_{sphere}.

In the previous study, m_{sphere} was determined with a relative uncertainty of 2.4×10^{-8} [4], which was reduced to 2.1×10^{-8} in this work. This improvement was achieved by the reduction of the uncertainty of V_{core}. One of the large uncertainty sources in the V_{core} measurement in the previous study was the interferogram analysis to measure the gaps d_1 and d_2. The gaps were determined from the extrema of the phase maps obtained by the phase-shifting interferometry. The extrema were determined by fitting the phase maps using the Zernike polynomials. From the residual of the fitting, the uncertainty contribution of the interferogram analysis to the diameter measurement was estimated to be 0.3 nm [4]. In this work, the uncertainty contribution was reduced to 0.1 nm by a rigorous alignment of the components of the

TABLE IV
UNCERTAINTY BUDGET OF THE MASS OF THE SPHERE IN VACUUM m_{sphere}

Uncertainty source	Relative standard uncertainty in m_{sphere}
Core volume, V_{core}	1.8×10^{-8}
Mass of the surface layer, m_{SL}	7.0×10^{-9}
Relative atomic mass of silicon, A_{r}(Si)	5.4×10^{-9}
Lattice parameter, a	5.5×10^{-9}
Mass deficit due to impurities and vacancies, m_{deficit}	3.8×10^{-9}
m_{sphere}	2.1×10^{-8}

TABLE V
RESULTS OF THE KILOGRAM REALIZATIONS BY NMIJ

Year	m_{sphere} / g	m_{core} / g	m_{SL} / g
2016 [4]	999.698 4571	999.698 3365	0.000 120 6
2020 (this work)	999.698 4383	999.698 3345	0.000 103 8

optical interferometer. This reduced the relative uncertainty of V_{core} from 2.0×10^{-8} to 1.8×10^{-8}. Details of the improvement are described in [19].

VI. MASS COMPARISON WITH TRANSFER STANDARDS

Two 1 kg weights made of the platinum-iridium alloy were used as transfer standards of NMIJ for the international comparison CCM.M-K8.2019. The masses of the weights were compared with that of AVO28-S5c realized in this work using a vacuum balance at NMIJ [16] in January 2020. The pilot laboratory, Bureau International des Poids et Mesures (BIPM), has already carried out mass comparisons among the transfer standards from all participants. Details of the mass comparisons are given in [24].

VII. COMPARISON WITH THE REALIZATION IN 2016

The sphere mass m_{sphere} is determined from the core mass m_{core} and the mass of the surface layer m_{SL}, as shown by (8). Table V shows m_{sphere}, m_{core}, and m_{SL} measured by NMIJ for the pilot study in 2016 [4] and those for CCM.M-K8.2019 in this work. As shown in Table V, m_{sphere} in this work is smaller than that in 2016 by 18.8 μg. This reduction was introduced by the decrease in m_{core} by 2.0 μg and the decrease in m_{SL} by 16.8 μg. The decrease in m_{SL} was mainly introduced by the decrease of the mass of the CL. In the realization, the surface characterization was performed after the volume measurement using the optical interferometer. In 2016, it was found that the surface layer was contaminated by fluorine, and the mass of the CL was estimated to be 37.7(5.9) μg [4]. The source of fluorine was estimated to be the sphere rotation mechanism of the optical interferometer, in which the sphere was lifted by a cylinder made of a resin containing fluorine when the sphere was rotated. Before the sphere volume measurement in this work, the cylinder was replaced by one made of a fluorine-free resin Poly Ether Ether Ketone (PEEK). Fluorine was not detected at all in the surface characterization in this work, and the mass of the carbonaceous CL was reduced to 19.6(3.8) μg.

TABLE VI
COMPARISON OF THE PARAMETERS USED IN THE KILOGRAM REALIZATIONS BY NMIJ

	In 2016 [4]	This work
h / 10^{-34} J s	6.626 070 040 [a]	6.626 070 15
R_∞ / 10^7 m^{-1}	1.097 373 156 8508(65) [a]	1.097 373 156 8160(21) [b]
A_{r}(e) / 10^{-4}	5.485 799 909 70(15) [a]	5.485 799 909 65(16) [b]
α / 10^{-3}	7.297 352 5664(17) [a]	7.297 352 5693(11) [b]
a / pm	543.099 6219(10)	543.099 623 80(97)

[a] Value in CODATA2014 [25]
[b] Value in CODATA2018 [8]

The change in m_{core} is much more complex. In the pilot study and this work, the values of some parameters used to determine m_{core} by (7) are different, as shown in Table VI.

A. Planck Constant and Other Fundamental Constants

The Planck constant h used for the realization in 2016 is the Committee on Data for Science and Technology (CODATA) 2014 recommend value [25] and is different from that used in this work. This difference increases m_{core} by 16.6 μg compared with m_{core} in 2016.

The Rydberg constant R_∞, the fine-structure constant α and the relative atomic mass of electron A_{r}(e) used for the realization in 2016 are the CODATA 2014 recommend values [25] and are different from those used in this work. These differences reduce m_{core} by 0.8 μg compared with m_{core} in 2016.

B. Lattice Parameter

As described in Section V, the lattice parameter a of AVO28-S5c used in 2016 is different from that in this work owing to the rigorous evaluation of the diffraction of the laser beam and the surface stress in the measurement of a using the XINT. This difference reduces m_{core} by 10.5 μg compared with m_{core} in 2016.

In summary, the above-described differences of the values of h, R_∞, α, A_{r}(e), and a increases m_{core} by 5.3 μg compared with m_{core} in 2016. The m_{core} in this work is smaller than that in 2016 by 2.0 μg, as shown in Table V. The net change in m_{core} between the two realizations was estimated to be about −7.3 μg. The cause of this change can be attributed to the core diameter measurement. The average core diameter in this work is smaller than that in 2016 by 0.2 nm, resulting in a decrease of about 7 μg in the core mass.

VIII. REPRODUCIBILITY OF THE REALIZATION

The reproducibility of the realization was examined using the national prototype of the kilogram of Japan. This prototype is a copy of the international prototype of the kilogram and was labeled No. 6 in 1889. The traceability of the mass of the No. 6

TABLE VII
MASS OF THE NO.6, NATIONAL PROTOTYPE OF THE KILOGRAM OF JAPAN

	March 2016	January 2020, this work
$m_{6,h}$ / g [a)]	1000.000 186(25)	1000.000 184(22)
$m_{6,\mathrm{IPK}}$ / g [b)]	1000.000 1880(105) [c)]	1000.000 1883(105) [c)]

[a)] The mass of the No. 6 based on the mass of AVO28-S5c realized by the XRCD method in [4] and in this study. The value of the Planck constant used for the realization in March 2016 is different from that used in this work as shown in Table VI.
[b)] The mass of the No. 6 based on the international prototype of the kilogram.
[c)] The mass was estimated on the assumption that the standard uncertainty of the mass of the IPK is 10 μg

to the international prototype of the kilogram was secured by the Extraordinary Calibration by BIPM in 2014, and the masses of the No. 6 in 2016 and 2020 were estimated on the basis of the international prototype of the kilogram using a model for compensating for mass increase of the No. 6 [26]. On the other hand, the mass of the No. 6 was determined on the basis of the mass of AVO28-S5c realized from h in this study using the vacuum balance in 2020. In addition, the mass of the No. 6 was determined in 2016 on the basis of the mass of AVO28-S5c realized for the pilot study [4]. The masses determined by the two methods are summarized in Table VII. The mass of the No. 6 based on the Planck constant $m_{6,h}$ in 2020 was smaller than that in 2016 by 2.0 μg. As described in Section VII, the values of some parameters used for the two realizations are different. Taking into account the differences, the net change of the mass of the No. 6 between the two realizations was estimated to be 7.3 μg. On the other hand, the mass of the No. 6 based on the international prototype of the kilogram $m_{6,\mathrm{IPK}}$ in 2020 was estimated to be larger than that in 2016 by 0.3 μg. The difference between the mass changes of the No. 6 estimated by the two different methods is, therefore, 7.6 μg. This difference is consistent with the net decrease in m_{core} described in Section VII and might be used as information to estimate the reproducibility of the realization by NMIJ. The realization of the kilogram from the Planck constant in this work is the second realization for NMIJ. The realization should, therefore, be repeated for a more rigorous estimation of the reproducibility.

IX. CONCLUSION

The international equivalence of the realization by NMIJ was confirmed in the key comparison CCM.M-K8.2019 [24]. In addition, the reproducibility of the realization was evaluated in this study. On the basis of these facts, NMIJ uses the realization technique to calibrate the primary mass standard of Japan in the future. Further reduction of the uncertainty of the realization is, therefore, necessary for accurate dissemination of mass standards from NMIJ. At present, the largest uncertainty source in the realization is the apparent volume measurement of the ^{28}Si-enriched sphere by the optical interferometer. As shown in Table I, the largest uncertainty source in the volume measurement is the phase correction due to the diffraction effect. To reduce the contribution from this uncertainty source, a new interferometer is being developed at NMIJ [9], [19]. The relative uncertainty of the volume measurement is expected to be reduced from 1.8×10^{-8} to 8×10^{-9} by the new interferometer. As a result of this improvement, the relative uncertainty of the realization of the kilogram will be reduced to 1.4×10^{-8}, corresponding to 14 μg for 1 kg.

ACKNOWLEDGMENT

The ^{28}Si-enriched sphere AVO28-S5c was used under the international collaboration to use the AVO28 crystal produced by the International Avogadro Coordination.

REFERENCES

[1] M. Stock, R. Davis, E. D. Mirandés, and M. J. T. Milton, "The revision of the Si—The result of three decades of progress in metrology," *Metrologia*, vol. 56, no. 2, Apr. 2019, Art. no. 022001.
[2] *Mise en Pratique for the Definition of the Kilogram in the SI*. Accessed: Mar. 4, 2021. [Online]. Available: https://www.bipm.org/utils/en/pdf/si-mep/SI-App2-kilogram.pdf
[3] *CCM Detailed Note on the Dissemination Process After the Redefinition of the Kilogram*. Accessed: Mar. 4, 2021. [Online]. Available: https://www.bipm.org/utils/common/pdf/CC/CCM/CCM_Note-on-dissemination-after-redefinition.pdf
[4] N. Kuramoto *et al.*, "Realization of the kilogram based on the Planck constant at NMIJ," *IEEE Trans. Instrum. Meas.*, vol. 66, no. 6, pp. 1267–1274, Jun. 2017.
[5] N. Kuramoto *et al.*, "Reproducibility of the realization of the kilogram based on the Planck constant by the XRCD method at NMIJ," in *Proc. Conf. Precis. Electromagn. Meas. (CPEM)*, Aug. 2020, pp. 1–2.
[6] M. Stock *et al.*, "A comparison of future realizations of the kilogram," *Metrologia*, vol. 55, no. 1, pp. T1–T7, 2018.
[7] Y. Azuma *et al.*, "Improved measurement results for the Avogadro constant using a ^{28}Si-enriched crystal," *Metrologia*, vol. 52, no. 2, pp. 360–375, 2015.
[8] *CODATA International Recommended 2018 Values of the Fundamental Physical Constants*. Accessed: Mar. 4, 2021. [Online]. Available: https://physics.nist.gov/cuu/Constants/index.html
[9] N. Kuramoto, L. Zhang, K. Fujita, S. Okubo, H. Inaba, and K. Fujii, "Volume measurement of a ^{28}Si-enriched sphere for a determination of the Avogadro constant at NMIJ," *IEEE Trans. Instrum. Meas.*, vol. 68, no. 6, pp. 1913–1920, Jun. 2019.
[10] N. Kuramoto, Y. Azuma, H. Inaba, and K. Fujii, "Volume measurements of ^{28}Si-enriched spheres using an improved optical interferometer for the determination of the Avogadro constant," *Metrologia*, vol. 54, no. 2, pp. 193–203, Apr. 2017.
[11] H. Inaba *et al.*, "Long-term measurement of optical frequencies using a simple, robust and low-noise fiber based frequency comb," *Opt. Exp.*, vol. 14, no. 12, pp. 5223–5231, 2006.
[12] H. Inaba *et al.*, "Frequency measurement capability of a fiber-based frequency comb at 633 nm," *IEEE Trans. Instrum. Meas.*, vol. 58, no. 4, pp. 1234–1240, Apr. 2009.
[13] L. Zhang, N. Kuramoto, Y. Azuma, A. Kurokawa, and K. Fujii, "Thickness measurement of oxide and carbonaceous layers on a ^{28}Si sphere by XPS," *IEEE Trans. Instrum. Meas.*, vol. 66, no. 6, pp. 1297–1303, Jun. 2017.
[14] K. Fujita, N. Kuramoto, Y. Azuma, S. Mizushima, and K. Fujii, "Surface layer analysis of a ^{28}Si-enriched sphere both in vacuum and in air by ellipsometry," *IEEE Trans. Instrum. Meas.*, vol. 66, no. 6, pp. 1283–1288, Jun. 2017.
[15] N. Kuramoto *et al.*, "Diameter comparison of a silicon sphere for the international Avogadro coordination project," *IEEE Trans. Instrum. Meas.*, vol. 60, no. 7, pp. 2615–2620, Jul. 2011.
[16] S. Mizushima, N. Kuramoto, L. Zhang, and K. Fujii, "Mass measurement of ^{28}Si-enriched spheres at NMIJ for the determination of the Avogadro constant," *IEEE Trans. Instrum. Meas.*, vol. 66, no. 6, pp. 1275–1282, Jun. 2017.
[17] G. Bartl, A. Nicolaus, E. Kessler, R. Schödel, and P. Becker, "The coefficient of thermal expansion of highly enriched ^{28}Si," *Metrologia*, vol. 46, no. 5, pp. 416–422, 2009.
[18] N. Kuramoto, K. Fujii, and K. Yamazawa, "Volume measurements of ^{28}Si spheres using an interferometer with a flat etalon to determine the Avogadro constant," *Metrologia*, vol. 48, no. 2, pp. S83–S95, Apr. 2011.
[19] Y. Ota, S. Okubo, H. Inaba, and N. Kuramoto, "Volume measurement of a ^{28}Si-enriched sphere to realize the kilogram based on the Planck constant at NMIJ," *IEEE Trans. Instrum. Meas.*, early access, Feb. 22, 2021, doi: 10.1109/TIM.2021.3061249.

[20] I. Busch *et al.*, "Surface layer determination for the Si spheres of the Avogadro project," *Metrologia*, vol. 48, no. 2, pp. S62–S82, Apr. 2011.
[21] S. Mizushima, "Determination of the amount of gas adsorption on SiO_2/Si(100) surfaces to realize precise mass measurement," *Metrologia*, vol. 41, no. 3, pp. 137–144, Jun. 2004.
[22] BIPM. *The International System of Units (SI)*. Accessed: Mar. 4, 2021. [Online]. Available: https://www.bipm.org/utils/common/pdf/si-brochure/SI-Brochure-9-EN.pdf
[23] G. Bartl *et al.*, "A new ^{28}Si single crystal: Counting the atoms for new kilogram definition," *Metrologia*, vol. 54, pp. 693–715, 2017.
[24] M. Stock *et al.*, "Report on the CCM key comparison of kilogram realizations CCM. M-K8. 2019," *Metrologia*, vol. 57, no. 1, p. 07030, 2020.
[25] P. J. Mohr, D. B. Newell, and B. N. Taylor, "CODATA recommended values of the fundamental physical constants: 2014," *Rev. Mod. Phys.*, vol. 88, no. 3, 2016, Art. no. 035009.
[26] S. Mizushima and K. Fujii, "Establishment of the platinum–iridium kilogram mass standards at NMIJ after the extraordinary calibrations," *Metrologia*, vol. 53, no. 2, pp. 787–799, Apr. 2016.

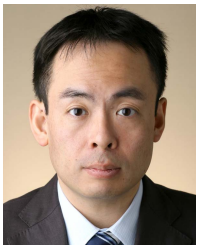

Naoki Kuramoto was born in Kanagawa, Japan, in 1971. He received the B.S., M.S., and Ph.D. degrees in chemistry from Saga University, Saga, Japan, in 1993, 1995, and 1998, respectively.

From 1995 to 1998, he was a Research Fellow with the Japan Society for the Promotion of Science. From 1998 to 1999, he was with the Tokyo University of Agriculture and Technology, Tokyo, Japan. In 1999, he joined the National Metrology Institute of Japan/the National Institute of Advanced Industrial Science and Technology (NMIJ/AIST), Tsukuba, Japan. He developed an optical frequency-scanning type laser interferometer for measuring the diameter of Si spheres. The Planck constant determined by Kuramoto *et al.* in 2017 was used as an input datum for the determination of the Planck constant in the present definition of the kilogram. He is currently the Leader of the Mass Standards Group. He also serves as the Coordinator of the International Avogadro Coordination (IAC) Project. His research interest includes the development of new mass measurement principles based on the new definition of the kilogram.

Shigeki Mizushima was born in Toyama, Japan, in 1972. He received the B.S. and M.S. degrees in physics from The University of Tokyo, Tokyo, Japan, in 1995 and 1997, respectively.

He is currently with the National Metrology Institute of Japan/the National Institute of Advanced Industrial Science and Technology (NMIJ/AIST), Tsukuba, Japan. His area of work includes mass and gravity measurements.

Lulu Zhang was born in Beijing, China, in 1968. She received the M.S. and Ph.D. degrees from Osaka University, Osaka, Japan, in 1995 and 1998, respectively.

From 1997 to 1998, she was a Fellow with the Japan Society for the Promotion of Science. From 1998 to 2004, she was a Post-Doctoral Researcher with the National Institute of Advanced Industrial Science and Technology (AIST), Tsukuba, Japan. She joined the National Metrology Institute of Japan (NMIJ), AIST, in 2004, where she is currently a Senior Research Scientist with the Surface and Nano-Analysis Section. Her research interest includes surface analysis and thickness metrology of thin films.

Kazuaki Fujita was born in Hyogo, Japan, in 1990. He received the B.S. and M.S. degrees in engineering from the Tokyo Institute of Technology, Tokyo, Japan, in 2013, 2015, respectively.

He joined the National Metrology Institute of Japan (NMIJ, the National Research Laboratory of Metrology)/the National Institute of Advanced Industrial Science and Technology (AIST), Tsukuba, Japan, in 2015. His research interest includes surface analysis for mass standards.

Sho Okubo was born in Tokyo, Japan, in 1984. He received the B.S., M.S., and Ph.D. degrees from Keio University, Yokohama, Japan, in 2007, 2009, and 2012, respectively. His doctoral work focused on high-resolution mid-infrared molecular spectroscopy.

He joined the National Metrology Institute of Japan (NMIJ), National Institute of Advanced Industrial Science and Technology (AIST), Tsukuba, Japan, in 2012. His research interests include optical frequency comb generation, control, and applications, in particular, spectroscopy using an optical frequency comb.

Dr. Okubo is a member of the Physical Society of Japan, the Japan Society of Applied Physics, and the Spectroscopical Society of Japan.

Hajime Inaba was born in Otaru, Japan, in 1969. He received the B.S., M.S., and Ph.D. degrees in applied physics from Hokkaido University Sapporo, Sapporo, Japan, in 1991, 1993, and 2004, respectively.

In 1993, he was with the National Research Laboratory of Metrology (NRLM), Tsukuba, Japan, where he worked on continuous-wave erbium-doped fiber lasers. Since 2001, he has been engaged in research on generation, control, and applications of optical frequency combs. He is currently a Research Scientist with the National Institute of Advanced Industrial Science and Technology (AIST), National Metrology Institute of Japan (NMIJ), Tsukuba.

Dr. Inaba is a member of the Japan Society of Applied Physics, and the Laser Society of Japan. He was a recipient of the Prize for Science and Technology from the Minister of Education, Culture, Sports, Science and Technology in 2008 and the Ichimura Science Awards in 2012.

Yasushi Azuma was born in Yamagata, Japan, in 1972. He received the B.S., M.S., and Ph.D. degrees in technology from Chiba University, Chiba, Japan, in 1995, 1997, and 2000, respectively. His doctoral work focused on the electronic structure and molecular orientation of ultrathin films of π conjugated molecules studied by multiple surface analysis technique.

He was a Research Fellow of the Japan Society for the Promotion of Science, from 1999 to 2000. He joined the National Metrology Institute of Japan/National Institute of Advanced Industrial Science and Technology, Tsukuba, Japan, in 2001. He is currently a Senior Research Scientist with the Surface and Nano Analysis Research Group. His research interest includes the development of thickness metrology and standard materials consisting of thin and multilayer films.

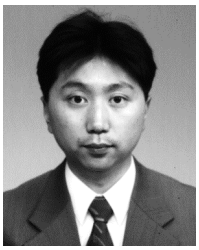

Akira Kurokawa was born in Ehime, Japan, in 1962. He received the B.S., M.S., and Ph.D. degrees in engineering from Osaka University, Suita, Japan, in 1985, 1987, and 1991, respectively. His doctoral work focused on ion beam-induced surface segregation.

After joining the Electrotechnical Laboratory (currently the National Institute of Advanced Industrial Science and Technology), Tsukuba, Japan, he has been working on the development of the silicon oxidation process with high-purity ozone gas and the uniform silicon dioxide thin film fabrication. He is currently a Chief Senior Researcher of the Nanomaterial Structure Analysis Research Group, National Metrology Institute of Japan, Tsukuba, Japan.

Yuichi Ota was born Tokyo, Japan, in 1986. He received the B.S. degree from Tohoku University, Sendai, Japan, in 2009, and the M.S. and Ph.D. degrees from The University of Tokyo, Kashiwa, Japan, in 2011 and 2014, respectively.

From 2011 to 2014, he was a Research Fellow of the Japan Society for the Promotion of Science. From 2014 to 2018, he was with the Institute for Solid State Physics, The University of Tokyo. In 2018, he joined the National Metrology Institute of Japan, National Institute of Advanced Industrial Science and Technology, Tsukuba, Japan.

Kenichi Fujii received the B.E., M.E., and Ph.D. degrees from Keio University, Yokohama, Japan, in 1982, 1984, and 1997, respectively. His doctoral work focused on the absolute measurement of the density of silicon crystals.

He joined the National Metrology Institute of Japan (NMIJ, formerly the National Research Laboratory of Metrology), Tsukuba, Japan, in 1984. From 1994 to 1996, he joined the National Institute of Standards and Technology (NIST), Gaithersburg, MD, USA, as a Guest Researcher of the Electricity Division to engage in the watt balance experiment. In 1988, he started an absolute measurement of the density of silicon crystals for the determination of the Avogadro constant. He developed a scanning-type optical interferometer for measuring the diameter of the silicon sphere.

Dr. Fujii is a member of the CODATA Task Group on Fundamental Constants. He serves as the Vice Chairperson of the Working Group on Density and Viscosity (WGDV) of the Consultative Committee for Mass and Related Quantities (CCM).